State and actuator fault estimation observer design integrated in a riderless bicycle stabilization system

Abstract

This paper deals with an observer design for Linear Parameter Varying (LPV) systems with high-order time-varying parameter dependency. The proposed methodology allows to design an observer in charge of the estimation of the actuator fault and the system state, considering measurement noise at the system outputs, which is as the main contribution for this paper. As a result, the actuator fault estimation is ready to be used in a Fault Tolerant Control (FTC) scheme, where the estimated state with reduced noise may be used to generate de control law. The effectiveness of the proposed methodology has been tested using a riderless bicycle model dependent on the translational velocity, where the control objective corresponds to the system stabilization towards the vertical position despite the variation of the translational velocity of the bicycle.

Keywords: LPV systems, parameter varying, actuator fault detection, actuator fault estimation, state estimation.

1. Introduction

The Linear-Parameter-Varying (LPV) modeling has represented, over the last few decades, a simple way to approach nonlinear dynamics. This representation allows the approximation of complex systems based on a set of

parameters whose value may change along the system trajectories and which are part of the original system. In addressing the LPV representation, several formulations exist: polytopic, Linear Fractional Transformation (LFT) and LPV affine. The polytopic LPV systems have been broadly studied because they provide a suitable representation computed as the combination of linear models —that approach the system behavior at a finite number of operating points— visualized as the vertices of a polytope (Poussot-Vasal et al., 2008; Rotondo et al., 2013). The LFT representation of LPV systems involves the separation between the varying and non-varying part of the model (Gonzalez et al., 2013). Finally, the affine formulation considers an infinite number of equilibrium points. Within the last case, there is an additional representation which involves dependency on multiple degree of the parameter varying: the polynomial LPV systems (Andreo et al., 2010; Gilbert et al., 2010). Such a particular formulation of LPV systems presents a difficult consideration: the stability analysis leads to problems related to parameter-varying Linear Matrix Inequalities (LMI). In other words, the main difficulty within the polynomial LPV systems corresponds to the solution of parameter-dependent LMI and, consequently, a less studied case. On the other hand, the continued growth of the control systems requires to maintain an acceptable level of reliability, whence the Fault-Tolerant-Control (FTC) (Zhang and Jiang, 2008) becomes relevant. In this direction, a very important issue corresponds to the estimation of the fault acting into the system. The reason comes intuitively: if the fault magnitude is known, then it is possible to take corrective actions to ensure the control objectives. Such corrective actions may involve the modification of the control gains or the addition of virtual actuator and/or

sensors. Further, in terms of control system design, it is highly desirable to compute a control law that contributes to a smooth and unforced operation of the system actuator, which could hardly be accomplished in the presence of noise at the system outputs. Thus, the main contribution of this paper corresponds to the design of an observer in charge of the actuator fault estimation along with the system state, with less noise than the one presentes at the system outputs. Thus, the proposed observer can be used in a FTC framework since the fault estimation and estimated states generate a control signal with less noise corruption.

In the LPV fault reconstruction literature, Alwi et al. (2012) proposed an observer applying the sliding mode methodology for fault estimation with application to a Boeing 747-100 LPV model with affine representation. In Patton and Klinkhieo (2010), fault estimation and LPV fault compensation are addressed, maintaining the control objectives, through the use of an affine LPV model of a two-link manipulator. Bara et al. (2000) deals with a state observer for affine LPV systems, with a solution computed as a linear combination between the parameters and their boundaries. Furthermore, for a winding machine system, a polytopic LPV sensor fault detection filter has been developed in Rodrigues et al. (2013). Although the works in these references are applied to LPV systems, the actuator fault estimation remains insufficiently explored in the polynomial LPV system framework. As a result, the design of the proposed observer is based on the LTI robust methodology extension to polynomial LPV systems, considering the stability characteristics for this kind of systems.

The paper structure is as follows: section 2 presents the definition of polyno-

mial LPV systems as well as its controllability and observability conditions, section 3 addresses the riderless bicycle model and its dynamical analysis and section 4 provides the preliminaries on the stabilization of the riderless polynomial LPV model. Section 5 presents the state and actuator fault estimation observer design, section 6 provides the controller design and section 7 addresses the observer and control gain computation. Finally, section 8 shows simulation results considering different types of actuator faults. Conclusions are presented in section 9.

2. Polynomial LPV systems

Consider the following dynamical system:

$$\begin{aligned} \dot{x} &= A(\zeta(t))x + B(\zeta(t))u \\ y &= C(\zeta(t))x \end{aligned} \tag{1}$$

where $x \in \mathbb{R}^n$, $u \in \mathbb{R}^p$ and $y \in \mathbb{R}^s$ correspond to the state,input and output (vector) variables, respectively. $A(\zeta(t))$, $B(\zeta(t))$ and $C(\zeta(t))$ represent parameter-dependent matrices of compatible dimensions. $\zeta(t) \in \mathbb{R}^m$ is the time-varying parameter vector. Normally, ζ is considered measurable and bounded, with a sufficiently smooth-time variation with bounded time ratio $\dot{\zeta}$, i.e. $\exists \nu, \mu > 0$ such that $\|\zeta(t)\| \leq \nu$ and $\|\dot{\zeta}(t)\| \leq \mu$.
If $A(\zeta(t))$, $B(\zeta(t))$ and $C(\zeta(t))$ adopt the form:

$$\chi(\zeta) = \chi_0 + \sum_{i=1}^{k} \sum_{j=1}^{m} \chi_{[(i-1)m]+j} \zeta(t)_j^i \tag{2}$$

for some $k \geq 1$, where χ_l, $l = 0, \ldots, km$, are matrices of compatible dimensions (depending the referred matrix $A(\zeta(t))$, $B(\zeta(t))$ or $C(\zeta(t))$), then

the state model (1) corresponds to a polynomial LPV system. As an example (from now on the term t will be omitted for practical reasons), consider $\zeta \in \mathbb{R}^2$, i.e. two time-varying parameters ζ_1 and ζ_2. With $m = 2$, the Ec. (2) will correspond to :

$$\chi(\zeta) = \chi_0 + \chi_1\zeta_1 + \chi_2\zeta_2 + \chi_3\zeta_1^2 + \chi_4\zeta_2^2 \tag{3}$$

As a result, the system dependency in the time-varying parameter vector will appear in polynomial form.

2.1. Controllability and observability

According to (Briat , 2008), the controllability and observability conditions for polynomial LPV systems can be seen as the extension for those criteria applied to Linear Time Invariant (LTI) systems. The polynomial LPV system (1) is controllable if:

$$rank[B(\zeta)\ \ A(\zeta)B(\zeta)\dots A(\zeta)^{n-1}B(\zeta)] = n\ \ \forall\ \zeta \leq \nu \tag{4}$$

In analogous way, a polynomial LPV the system will be observable if:

$$rank\begin{bmatrix} C(\zeta) \\ C(\zeta)A(\zeta) \\ \vdots \\ C(\zeta)A(\zeta)^{n-1} \end{bmatrix} = n\ \ \forall\ \zeta \leq \nu \tag{5}$$

3. The Riderless bicycle model and its dynamical analysis

The riderless bicycle dynamics can be formulated in terms of a general frame which includes a rigid body, a front frame composed by the handle and the

tires. The general representation (Schwab et al., 2005) for this system is given as:

$$Q\ddot{q} + vW\dot{q} + (gE_0 + v^2E_1)q = f \tag{6}$$

where $q \in \mathbb{R}^2$ is the angular position vector containing the roll angle ϕ and the handlebar angle δ, i.e. $q = [\phi \ \ \delta]^T$, $f \in \mathbb{R}^2$ is the input force vector composed by the torque applied to the general frame T_ϕ and handlebar T_δ, i.e. $f = [T_\phi \ T_\delta]^T$ as shown in Figure 1. In Ec. (6) Q and W are the mass and damping constant matrices, respectively; E_0 and E_1 are stiffness coefficient matrices, and g is the gravity acceleration. The referred matrices, Q, W, E_0 and E_1, are related with the physical properties of the prototype and the effects of its interaction with the environment. The motion equation (6) has been validated for small variations around ϕ and δ, considering the bicycle at a vertical position (Schwab et al., 2005).

FIGURE 1

Defining the state vector as $x = \left[\phi \ \ \delta \ \ \dot{\phi} \ \ \dot{\delta}\right]^T$, the translational velocity of the bicycle as the time-varying parameter, i.e. $\zeta = v$, and taking the torque applied to the handlebar T_δ as a unique input force, the state space representation for (6) can be expressed as:

$$\begin{aligned} \dot{x} &= A(v)x + Bu \\ y &= Cx \end{aligned} \tag{7}$$

Where (Andreo et al. (2010)):

$$A(v) = \begin{bmatrix} 0 & 0 & 1 & 0 \\ 0 & 0 & 0 & 1 \\ 13.67 & 0.225 - 1.319v^2 & -0.164v & -0.552v \\ 4.857 & 10.81 - 1.125v^2 & 3.621v & -2.388v \end{bmatrix} B = \begin{bmatrix} 0 \\ 0 \\ -0.339 \\ 7.457 \end{bmatrix}$$
$$C = \begin{bmatrix} 0 & 1 & 0 & 0 \\ 0 & 0 & 1 & 0 \end{bmatrix} \tag{8}$$

It can be seen that the matrix $A(v)$ is velocity-dependent and it can be rewritten as $A(v) = A_0 + A_1 v + A_2 v^2$, which is consistent with Ec. (2). The Figure 2 shows the open-loop eigenvalues (of $A(v)$) as a function of the varying parameter v, as a reference to establish the open-loop eigenvalues as the parameter varying v changes. It is worth to note that the open-loop criterion, since LPV systems are related to Linear Time Varying systems (LTV), is not a sufficient condition for determine the stability of the system.

FIGURE 2

3.1. Controllability and observability conditions

The controllability and observability criteria for the LPV riderless bicycle model can be computed using (4) and (5), respectively, considering the following procedure (where $|\cdot|$ is used to denote the determinant of a matrix):

$$\begin{aligned} |\Lambda_c(v)| &= |[B \;\; A(v)B \;\; A(v)^2 B \;\; A(v)^3 B]| \\ |\Lambda_c(v)| &= -5806.5321v^4 + 19463.1274v^2 - 22.3115 \end{aligned} \tag{9}$$

Solving for v and taking the positive values, the loss of controllability condition occurs when v lies in the following translational velocity set:

$$v \in \mathbb{R} = \{0.03386, 1.8305\} \Rightarrow \det(\Lambda_c) = 0 \tag{10}$$

The observability condition, meanwhile, can be computed from the transpose of Ec. (5), since $rank[Q] = rank[Q^T]$. Let us point out that Ec. (5) will result in a rectangular matrix, by considering the system matrices defined in Ec. 8. As a result, the transpose of (5) referred from now on as $\Lambda_o(v)$ is:

$$\Lambda_o(v) = \begin{bmatrix} 0 & 0 & 0 & 13.67 & 4.857 \\ 1 & 0 & 0 & 0.225 - 1.319v^2 & 10.81 - 1.125v^2 \\ 0 & 1 & 0 & -0.164v & 3.621v \\ 0 & 0 & 1 & -0.552v & -2.388v \end{bmatrix}$$
$$\begin{bmatrix} -4.922v & 37.9v & 187.961 - 26.520v^2 \\ 0.837v^3 - 6v & -2.089v^3 - 24.996 & 2.5v^4 - 17.758v^2 + 5.51 \\ 13.67 - 1.971v^2 & 4.857 - 9.240v^2 & 0.648v^3 - 6.350v \\ 0.089v^2 + 0.225 & 2.578v^2 + 10.81 & 1.711v^3 - 14.087v \end{bmatrix} \quad (11)$$

In order to compute $rank[\Lambda_o(v)] = rank[\Lambda_o(v)^T]$, since it corresponds to a rectangular parameter-varying dependent matrix, the procedure begins with a non-zero determinant operation considering a square matrix with $n - 1$ dimension. Once the previously has been solved, the procedure continues by adding the resting rows and columns in order to obtain square matrices of n dimension. For each one of those square matrices, the determinant should be computed (the determinant operation will result in an equation involving the time-varying parameter v). Thus, for all v such that $rank[\Lambda_o(v)] \neq n$, and consequently the LPV model is not be observable. From Ec. (11), the $n - 1 \times n - 1$ square matrix considered corresponds to a identity matrix formed by the rows $2 - 4$ and columns $1 - 3$. By following the mentioned procedure, incorporating the row 1 and column 4:

$$\Lambda_{o1} = \begin{bmatrix} 0 & 0 & 0 & 13.67 \\ 1 & 0 & 0 & 0.225 - 1.319v^2 \\ 0 & 1 & 0 & -0.164v \\ 0 & 0 & 1 & -0.552v \end{bmatrix} = \begin{bmatrix} 0_{1\times 3} & 13.67 \\ I_3 & V_1 \end{bmatrix} \tag{12}$$

where I_3 is the identity matrix $\in \mathbb{R}^{3\times 3}$ and $V_1 \in \mathbb{R}^{3\times 1}$ whit $|\Lambda_{o1}| = -13.67$. Incorporating the row 1 and column 5:

$$\Lambda_{o2} = \begin{bmatrix} 0 & 0 & 0 & 4.857 \\ 1 & 0 & 0 & 10.81 - 1.125v^2 \\ 0 & 1 & 0 & 3.621v \\ 0 & 0 & 1 & -2.388v \end{bmatrix} = \begin{bmatrix} 0_{1\times 3} & 4.5857 \\ I_3 & V_2 \end{bmatrix} \tag{13}$$

in which case $|\Lambda_{o2}| = -4.857$. In analogous way, matrices Λ_{o3}, Λ_{o4} and Λ_{o5} were found to be:

$$\begin{gathered} \Lambda_{o3} = \begin{bmatrix} 0_{1\times 3} & -4.922v \\ I_3 & V_3 \end{bmatrix} \quad \Lambda_{o4} = \begin{bmatrix} 0_{1\times 3} & 37.9v \\ I_3 & V_4 \end{bmatrix} \\ \Lambda_{o5} = \begin{bmatrix} 0_{1\times 3} & 187.961 - 26.520v^2 \\ I_3 & V_5 \end{bmatrix} \end{gathered} \tag{14}$$

By computing the respective determinants of these last three matrices, it can be concluded that the riderless bicycle LPV model is observable $\forall\, v$, since there is not a coincident v value in the solutions. As a result, the controllability and observability analysis allow to define the translational velocity interval for the bicycle for practical purposes as $\Phi = [0.5, 1.7]$ m/s.

4. Preliminary on the stabilization of a riderless bicycle

The control objective is to maintain the vertical position of the bicycle through a torque applied to the handle-bar axis T_δ despite a variant translational velocity v. Consider the system (7) with measurement noise and an additive actuator fault:

$$\begin{aligned} \dot{x} &= A(v)x + Bu + B_f f_a \\ y &= Cx + Dz \end{aligned} \tag{15}$$

where the matrix B_f considers the columns of B associated with the actuator under fault condition and f_a the fault magnitude vector. D and z represents the noise matrix and its magnitude, associated to the outputs of the system. In order to estimate the state x and the fault magnitude f_a an observer with the following structure is proposed:

$$\begin{aligned} \dot{\hat{x}} &= A(v)\hat{x} + Bu + B_f\hat{f}_a + K_0(v)(y - \hat{y}) \\ \dot{\hat{f}}_a &= L_0(v)(y - \hat{y}) \\ \hat{y} &= C\hat{x} \end{aligned} \tag{16}$$

where $K_0(v)$ and $L_0(v)$ are the time-varying observer gains. The objective is to design the observer (16) in order to provide the fault estimation $\hat{f}$ as well as the system state, minimizing the measurement noise presented at the system outputs. To reach the control objective, consider a control law:

$$u = T_\delta = k(v)\hat{x} \tag{17}$$

where $k(v)$ corresponds to the parameter-dependent control gains and $\hat{x}$ represents the state estimated by the observer (16). In order to analyze the dynamical behaviour of the stabilization system for the riderless bicycle model,

consider the dynamics of the state estimation error $e_e = x - \hat{x}$ along with estimation error for the actuator fault $e_f = f_a - \hat{f}_a$:

$$\begin{aligned} \dot{e_e} &= A(v)x + Bu + B_f f_a - (A(v)\hat{x} + Bu + B_f \hat{f}_a + K_0(v)(y - \hat{y})) \\ &= (A(v) - K_0(v)C)e_e + B_f e_f - K_0 D z \\ \dot{e_f} &= \dot{f}_a - L_0(v)(y - \hat{y}) \\ &= \dot{f}_a - L_0(v)Ce_e - L_0 D z \end{aligned} \tag{18}$$

Using the control law (17) in terms of the state estimation error e_e:

$$u = T_\delta = k(v)\hat{x} = k(v)(x - e_e) \tag{19}$$

the closed-loop system can be computed as follows:

$$\dot{x} = (A(v) + Bk(v))x - Bk(v)e_e + B_f f_a \tag{20}$$

As a result, the estimation errors e_e, e_f and the closed-loop system can be represented in matrix form as follows:

$$\begin{bmatrix} \dot{x} \\ \dot{e_e} \\ \dot{e_f} \end{bmatrix} = \begin{bmatrix} A(v) + Bk(v) & -Bk(v) & 0 \\ 0 & A(v) - K_0(v)C & B_f \\ 0 & -L_0(v)C & 0 \end{bmatrix} \begin{bmatrix} x \\ e_e \\ e_f \end{bmatrix} + \begin{bmatrix} B_f & 0 & 0 \\ 0 & -K_0(v)D & 0 \\ 0 & -L_0(v)D & I \end{bmatrix} \begin{bmatrix} f_a \\ z \\ \dot{f}_a \end{bmatrix} \tag{21}$$

From Ec. (21) the accomplishment of the separability principle can be concluded. The separability principle addresses the dynamical conditions to be

fulfilled in such way that the observer and control design can be done independently. To explain the previous, let us point out that through the observer gain $k_0(v)$ the state estimation error e_e involved in the closed-loop system (term $-Bk(v)$) will be $e_e \to 0$ as $t \to \infty$, consequently, the control design can be realized from the remaining term $A(v) + Bk(v)$. The observer, in turn, will be able to provide the fault estimation $\hat{f}_a$ by designing $L_0(v)$ such that $e_f \to 0$ as $t \to \infty$. The main issue in (21), corresponds to how to deal with the effects referred to the measurement noise z and the fault f_a, within the estimation errors dynamics and the closed-loop system. Whit this in mind, the observer design should consider a procedure capable to guarantee the observer stability despite on the fault and measurement noise magnitude. For this to be achieved, the conditions $f_a = 0$ and $f_a \neq 0$ should be taken in account in the observer design, issue addressed in the present article as the extension procedure existing in LTI systems to polynomial LPV systems. The guarantee of the observer stability despite on the fault magnitude and measurement noise is considered la main contribution of the present work.

5. Observer design: Stability

To begin with the observer design, consider the error estimation dynamics $\dot{e}_e$ and $\dot{e}_f$ (18) involved in the observer (16), represented in matrix form as follows.

$$\begin{bmatrix} \dot{e_e} \\ \dot{e_f} \end{bmatrix} = \begin{bmatrix} A(v) - K_0(v)C & B_f \\ -L_0(v)C & 0 \end{bmatrix} \begin{bmatrix} e_e \\ e_f \end{bmatrix} + \begin{bmatrix} -K_0(v)D & 0 \\ -L_0(v)D & I \end{bmatrix} \begin{bmatrix} z \\ \dot{F}_a \end{bmatrix} \tag{22}$$

Defining the vectors $\Delta = [e_e \ e_f]^T$ and $\Psi = \left[z \ \dot{f}_a\right]^T$, Eq. (22) can be rewritten in compact form as $\dot{\Delta} = \tilde{A}(v)\Delta + \tilde{b}\Psi$ with:

$$\tilde{A}(v) = \begin{bmatrix} A(v) - K_0(v)C & B_f \\ -L_0(v)C & 0 \end{bmatrix} \qquad \tilde{b} = \begin{bmatrix} -K_0(v)D & 0 \\ -L_0(v)D & I \end{bmatrix} \tag{23}$$

To ensure the state and fault estimation error convergence, a parameter-varying Lyapunov function (Rugh and Shamma, 2000) is considered $V(\Delta, v) = \Delta^T P(v)\Delta$ where $P(v)$ denotes a symmetric positive definite matrix. In order to guarantee $\Delta \to 0$ as $t \to \infty$, it is necessary to solve $\dot{V}(\Delta, v) < 0, \forall \Delta \in \mathbb{R}^n, \forall v \in \Phi$. As a result, the problem for state and fault estimation is reduced to find two parameter-dependent observer gains $K_0(v)$ and $L_0(v)$ such that the asymptotic convergence of Δ is accomplished if $\Psi = 0$ and the error vector Δ be bounded if $\Phi \neq 0$. Both conditions can be formulated in mathematical terms as:

$$\begin{aligned} \Delta \to 0 \quad \text{as} \quad t \to \infty \qquad & if \ \ \Psi = 0 \\ ||\Delta||_{Q_\Delta} \leqslant (\varsigma(v))^2 ||\Psi||_{Q_\Psi} \qquad & if \ \ \Psi \neq 0 \end{aligned} \tag{24}$$

where Q_Δ and Q_Ψ are positive-defined matrices, $\|\Delta\|_{Q_\Delta} = \Delta^T Q_\Delta \Delta$, $\|\Psi\|_{Q_\Psi} = \Psi^T Q_\Psi \Psi$ and $\varsigma(v)$ is the parameter-varying attenuation level. The expressions in (24) are fulfilled if:

$$\dot{V}(\Delta, v) + \Delta^T Q_\Delta \Delta - (\varsigma(v))^2 \Psi^T Q_\Psi \Psi < 0 \tag{25}$$

which in turn, corresponds to:

$$\begin{gathered}\Delta^T P(v)(\tilde{A}(v)\Delta + \tilde{b}\Psi) + \tfrac{d}{dt}(\Delta^T P(v))\Delta + \Delta^T Q_\Delta \Delta - (\varsigma(v))^2 \Psi^T Q_\Psi \Psi < 0 \\ \Delta^T P(v)(\tilde{A}(v)\Delta + \tilde{b}\Psi) + \Delta^T \dot{v}\tfrac{\partial P(v)}{\partial v}\Delta + (\tilde{A}(v)\Delta + \tilde{b}\Psi)^T P(v)\Delta + \\ \Delta^T Q_\Delta \Delta - (\varsigma(v))^2 \Psi^T Q_\Psi \Psi < 0 \\ \Delta^T P(v)\Delta + \Delta^T P(v)\tilde{b}\Psi + \Delta^T \dot{v}\tfrac{\partial P(v)}{\partial v}\Delta + \Delta^T \tilde{A}(v)^T P(v)\Delta + \Psi^T \tilde{b}^T P(v)\Delta + \\ \Delta^T Q_\Delta \Delta - (\varsigma(v))^2 \Psi^T Q_\Psi \Psi < 0\end{gathered} \tag{26}$$

In the inequality (26) is important to stand the significance of the $\Delta^T \dot{v}\frac{\partial P(v)}{\partial v}\Delta$ term. In LPV framework, the stability analysis considers the parameter varying velocity, which, in this particular case, corresponds to the bicycle translational acceleration. The previous is an important characteristic for the LPV system stability. Carry on with the observer design, Ec. (26) can be represented as:

$$\begin{bmatrix} \Delta \\ \Psi \end{bmatrix}^T \begin{bmatrix} P(v)\tilde{A}(v) + \tilde{A}(v)^T P(v) + \dot{v}\frac{\partial P(v)}{\partial v} + Q_\Delta & P(v)\tilde{b} \\ \tilde{b}^T P(v) & -(\varsigma(v))^2 Q_\Psi \end{bmatrix} \begin{bmatrix} \Delta \\ \Psi \end{bmatrix} < 0 \tag{27}$$

As a result, the estimation error convergence will be accomplished if the parameterized LMI:

$$\begin{bmatrix} P(v)\tilde{A}(v) + \tilde{A}(v)^T P(v) + \dot{v}\frac{\partial P(v)}{\partial v} + Q_\Delta & P(v)\tilde{b} \\ \tilde{b}^T P(v) & -(\varsigma(v))^2 Q_\Psi \end{bmatrix} < 0 \tag{28}$$

is feasible with $P(v) = P(v)^T > 0$. In order to solve (28) a brief modification should be performed:

$$\begin{aligned}\tilde{A}(v) &= \tilde{A}_1(v) - K_s(v)C_1 \\ &= \begin{bmatrix} A(v) & B_f \\ 0 & 0 \end{bmatrix} - \begin{bmatrix} K_0(v) \\ L_0(v) \end{bmatrix} [C \;\; 0] \end{aligned} \tag{29}$$

$$\begin{aligned}\tilde{b} &= - \;\; K_s(v)\tilde{b}_1 + C_2 \\ &= \quad - \begin{bmatrix} K_0(v) \\ L_0(v) \end{bmatrix} [D \;\; 0] + \begin{bmatrix} 0 & 0 \\ 0 & I \end{bmatrix} \end{aligned} \tag{30}$$

where I is the identity matrix of appropriated dimensions. The previous modification is made in order to eliminate the bilinear condition $P(v)K_0(v)$ and $P(v)L_0(v)$. Further, by making $K_{fo}(v) = P(v)K_s(v)$ and $M(v) = (\varsigma(v))^2$, the following is proposed.

Proposition I: The observer (16) will provide the fault and state estimation considering the state estimation error $e_e \to 0$ as $t \to \infty$ if $\Psi = 0$ and bounded by a factor $\varsigma(v)$ when $\Psi \neq 0$ if:

$$\begin{bmatrix} \kappa(v) + Q_\Delta & -K_{fo}(v)\tilde{b}_1 + P(v)C_2 \\ -\tilde{b}_1^T K_{fo}(v)^T + C_2^T P(v) & -M(v)Q_\Psi \end{bmatrix} < 0 \tag{31}$$

is feasible with $\kappa(v) = P(v)\tilde{A}_1(v) - K_{fo}(v)C_1 + \tilde{A}_1(v)^T P(v) - C_1^T K_{fo}(v)^T + \dot{v}\frac{\partial P(v)}{\partial v}$, $P(v) = P(v)^T > 0$, $[K_0(v) \;\; L_0(v)]^T = K_s(v) = P(v)^{-1}K_{fo}(v)$ and $\varsigma(v) = \sqrt{M(v)}$.

6. Controller Design

The following control law is proposed:

$$u = k(v)\hat{x} = \left[k\phi(v) \;\; k\delta(v) \;\; k\dot{\phi}(v) \;\; k\dot{\delta}(v)\right] \hat{x} \tag{32}$$

where the $k(v)$ is the parameter-varying control gain and $\hat{x}$ is provided by the observer given in (16). Forming the closed-loop system in fault-free case:

$$\dot{x} = (A(v) + Bk(v))x - Bk(v)e_e + B_f f_a \tag{33}$$

under the consideration that the solution of (31) guarantees the fault and state estimation error convergence as well as the effect of the actuator fault within the estimation, it is only necessary to design the control gain $k(v)$ such that $x \to 0$ when $t \to \infty$ considering $A(v) + Bk(v)$ in Eq. (33). For this to be achieved, the controller design considers a parameter-dependent Lyapunov function $V(x, v) = x^T Q(v)x$ with a derivative term:

$$\dot{V}(x, v) = Q(v)(A(v) + Bk(v)) + (A(v) + Bk(v))^T Q(v) + \dot{v}\frac{\partial Q(v)}{\partial v} < 0 \tag{34}$$

for some $Q(v) = Q(v)^T > 0$. Since the inverse of a symmetric and positive-definite matrix is symmetric and positive-definite, performing the pre-multiplication and post-multiplication operation in (34) by $Q(v)^{-1}$:

$$\begin{gathered}(A(v) + Bk(v))Q(v)^{-1} + Q(v)^{-1}(A(v) + Bk(v))^T + \dot{v}Q(v)^{-1}\frac{\partial Q(v)Q(v)^{-1}}{\partial v} < 0 \\ A(v)Q(v)^{-1} + Bk(v)Q(v)^{-1} + Q(v)^{-1}A(v)^T + Q(v)^{-1}k(v)^T B^T + \\ \dot{v}Q(v)^{-1}[\frac{\partial Q(v)}{\partial v}Q(v)^{-1} + Q(v)\frac{\partial Q(v)^{-1}}{\partial v}] < 0\end{gathered} \tag{35}$$

let us point out that:

$$\begin{gathered}\dot{v}Q(v)^{-1}[\frac{\partial Q(v)}{\partial v}Q(v)^{-1} + Q(v)\frac{\partial Q(v)^{-1}}{\partial v}] = \dot{v}Q(v)^{-1}\frac{\partial Q(v)}{\partial v}Q(v)^{-1} + \dot{v}\frac{\partial Q(v)^{-1}}{\partial v} = 0 \Rightarrow \\ \dot{v}Q(v)^{-1}\frac{\partial Q(v)}{\partial v}Q(v)^{-1} = -\dot{v}\frac{\partial Q(v)^{-1}}{\partial v}\end{gathered} \tag{36}$$

combining (35) and (36) $\dot{V}((x, v)) < 0$ will corresponds to:

$$A(v)Q(v)^{-1} + Bk(v)Q(v)^{-1} + Q(v)^{-1}A(v)^T + Q(v)^{-1}k(v)^T B^T + \dot{v}Q(v)^{-1} - \dot{v}\frac{\partial Q(v)^{-1}}{\partial v} < 0 \tag{37}$$

Finally, by making $X(v) = Q(v)^{-1}$ and $Y(v) = k(v)X(v)$ in order to retrieve the bilinear condition $k(v)X(v)$, the following LMI is obtained:

$$A(v)X(v) + BY(v) + X(v)^T A(v)^T + Y(v)^T B^T - \dot{v}\frac{\partial X(v)}{\partial v} < 0 \tag{38}$$

As a result, the asymptotic stability is guaranteed if the LMI (38) is solvable with $X(v) = X(v)^T > 0$. The final solution for the control gain is computed by:

$$k(v) = Y(v)X(v)^{-1} \tag{39}$$

7. Observer gain and control gain computation

The previous LMI restrictions can be seen as a set of parameter-varying LMI due to the translational velocity. The methods to solve this kind of problems are relaxation (Tuan and Apkarian, 1999), sum of Squares (Prajna and Wu, 2005) and discretization (Rugh and Shamma, 2000). In this paper the discretization method was used. The method is based on a discretization for the varying-parameter range using a difference approximation for the derivative term. Once the discrete solution has been computed, an interpolation method is used to generate the continuous one. The final LMI set to be solved for the controller gains corresponds to:

$$A(jh)X(jh) + BY(jh) + X(jh)^T A(jh)^T + Y(jh)B^T \pm \dot{v}\frac{Y(jh+h)-Y(jh)}{h} < 0$$
$$X(jh) = X(jh)^T > 0 \tag{40}$$

and for Proposition 1:

$$\begin{bmatrix} \kappa(jh) + Q_\Delta & -K_{fo}(jh)\tilde{b}_1 + P(jh)C_2 \\ -\tilde{b}_1^T K_{fo}(jh)^T + C_2^T P(jh) & -M(jh)Q_\Psi \end{bmatrix} < 0 \tag{41}$$

where $\kappa(jh) = P(jh)\tilde{A}_1(jh) - K_{fo}(jh)C_1 + \tilde{A}_1(jh)^T P(jh) - C_1^T K_{fo}(jh)^T \pm \dot{v}\frac{P(jh+h)-P(jh)}{h}$, $P(jh) = P(jh)^T > 0$, $K_s(jh) = P(jh)^{-1}K_{fo}(jh)$ and $\varsigma(jh) = \sqrt{M(jh)}$.

For the controller and observer design, a LMI region (Chilali and Gahinet, 1996) has been considered. In this context, the closed-loop eigenvalues, as a result of the control gains, will be allocated to the left side of the β_c value within the left complex plane by solving:

$$A(jh)X(jh) + BY(jh) + X(jh)^T A(jh)^T + Y(jh)B^T + 2X(jh)\beta_c < 0$$
$$X(jh) = X(jh)^T > 0 \tag{42}$$

The LMI region for the observer, on the other hand, will be defined by the parameter β_o and the following LMI:

$$\begin{bmatrix} \tilde{\kappa}(jh) + Q_\Delta + 2\beta_o P(jh) & -K_{fo}(jh)\tilde{b}_1 + P(jh)C_2 \\ -\tilde{b}_1^T K_{fo}(jh)^T + C_2^T P(jh) & -M(jh)Q_\Psi + 2\beta_o P(jh) \end{bmatrix} < 0 \tag{43}$$

where $\tilde{\kappa}(jh) = P(jh)\tilde{A}_1(jh) - K_{fo}(jh)C1 + \tilde{A}_1(jh)^T P(jh) - C1^T K_{fo}(jh)^T$.

In Eqs. (40)-(43), $j = 1, 2, ..., N$ is the gridding varying-parameter space and $h > 0$ the step width.

8. Simulation results

8.1. Control and observer gains: Solutions

The LMI set (40)-(43) was solved using $h = 0.02$, $N = 60$, and $\dot{v} = 0.05$ with YALMIP Toolbox (Lofberg et al., 2009) and MATLAB. The observer gains were computed considering $Q_\Delta = 1e^{-3}I$, $Q_\Psi = 750I$ and $\beta_o = 6$ in Ecs. (41)-(43), solved simultaneously. The interpolated observer gains corresponds to the 3 order function as follows:

$$K_s(v) = ZF3v^3 + ZF2v^2 + ZF1v + ZF0 \tag{44}$$

$$ZF3 = \begin{bmatrix} -8.899 & 4.481 \\ -3.589 & 2.486 \\ -2.327 & 1.911 \\ -17.585 & -10.529 \\ -14.965 & -17.049 \end{bmatrix} \quad ZF2 = \begin{bmatrix} 11.555 & -9.530 \\ -5.491 & -3.120 \\ 20.876 & -8.127 \\ 20.132 & 135.237 \\ 20.385 & 149.398 \end{bmatrix} \tag{45}$$

$$ZF1 = \begin{bmatrix} 22.240 & 7.315 \\ -7.723 & 0.558 \\ -41.298 & 11.004 \\ -799.597 & -217.092 \\ -437.676 & -242.273 \end{bmatrix} \quad ZF0 = \begin{bmatrix} 38.508 & 28.576 \\ 137.35127 & 0.280 \\ 7.818 & 26.794 \\ 2282.818 & 13.078 \\ 1338.391 & 3.758 \end{bmatrix} \tag{46}$$

For the control gains the LMI region considered was defined by $\beta_o = 1$. The solution, by solving (40) and (42) simultaneously, interpolated to functions of 4 order, were found to be:

$$k(v)^T = \begin{bmatrix} -79.0188 & 283.6894 & -234.4882 & -165.4273 & 262.0917 \\ -3.6333 & 10.3396 & -1.5758 & -22.6184 & 15.8127 \\ -22.1225 & 79.8812 & -68.4279 & -41.8261 & 70.3465 \\ 0.3839 & -3.1946 & 8.6688 & -10.3002 & 3.9232 \end{bmatrix} \begin{bmatrix} v^4 \\ v^3 \\ v^2 \\ v \\ 1 \end{bmatrix} \tag{47}$$

The eigenvalues corresponding to the estimation error matrix (29) are displayed in Figure 3. The real and imaginary part of the observer error eigenvalues are presented in Figure 3a), the real part of the eigenvalues in function of v in Figure 3b) and the parameter-varying attenuation level $\varsigma(jh)$ for the Eq. (24) in Figure 3c). The error convergence of state and fault estimation can be concluded from Figure 3.

FIGURE 3

Figure 4 shows the controller gains. The **asterisks** corresponds to the discrete values computed by solving the LMI (40) and (42), the continuous line, meanwhile, was obtained by using Eq. (47).

FIGURE 4

The closed-loop eigenvalues for $A(v) + Bk(v)$ in Ec. (33) are presented in Figure 5, concluding with the system stabilization $\forall v \in \Phi$ despite on a decreasing or creasing translational velocity.

FIGURE 5

8.2. Non-faulty case closed-loop simulation

Once the observer and controller gains have been computed, the simulation of the system (15) by using the control law (32) and the estimated $\hat{x}$ from (16) can be carried out. Gaussian noises z_1 with mean value 0 and variance $5e^{-3}$ and z_2 with mean 0 and variance $3e^{-3}$ and $D = 0.2I$ for (15) were considered, while applying initial conditions $x = [0 \;\; 0.1 \;\; -0.04 \;\; 0]^T$ and $\hat{x} = [0 \;\; 0.075 \;\; -0.02 \;\; 0]^T$ were taken. Figure 6 show the response of the controlled system with a translational velocity from 1.7 to 1.35 m/s (see Figure 6d). Figures 6a) and 6b) present the real and the estimated outputs y_δ and $y_{\dot{\phi}}$ showing the effectiveness of the proposed observer, able to compute the state estimation minimizing the measurement noise.

FIGURE 6

The control law, the roll angle estimated $\dot{\phi}$ and, the velocity for the handlebar $\dot{\delta}$ can be seen in 6c), 6e) and 6f), respectively. Let us point out that the LPV riderless bicycle model is valid for small variation around ϕ and δ, which should be consistent with the closed-loop state magnitude. With the previous in mind, the measurement noise presented at the system outputs have a magnitude of approximately ± 0.04 rad. or ± 2.29 degrees, which is a considerable noise with respect to the LPV model characteristics. Despite this fact, the proposed observer provides a state estimation in order to build the control law with less noise, which in turn will contribute to the smooth operation of the actuator.

8.3. Closed-loop simulation with BIAS actuator fault

This section shows the performance of the closed loop system by considering a BIAS actuator fault in the system (15). For this simulation, similar initial conditions were considered as in the previous case. Figures 7 and **??** present the results for a BIAS faulty case $F_a = 0.25$ at $t = 2.5$ s. The real and reconstructed outputs for the system are depicted in Figure 7a), whence one can see the fault occurrence and its implication in the closed-loop system. Figure 7a) displays a deviation from the bicycle equilibrium point in y_δ caused by the applied BIAS fault magnitude, where the referred output finishes at 1 rad. equivalent to a 5.73 degrees. The translational velocity variation is displayed in Figure 7d).

FIGURE 7

Finally, let us point out that $\dot{v} = |\frac{1.7-1.35}{0-7}| = 0.05$ (see Figure 7d), according to the stipulated value used to compute the control and observer gains. The control law T_δ, in turn, is depicted in Figure 7c). The estimated and the real fault are presented in Figure 8. It is seen that the fault estimation converges correctly in approximately $t = 0.5$ seg. Under the consideration that the translational velocity is changing its value continuosly, the actuator fault estimation error $e_f = f_a - \hat{f}_a$ stay close to 0, once the fault estimation has been estimated correctly.

FIGURE 8

8.4. Closed-loop simulation with a loss of effectiveness in the actuator

In this simulation, a loss of effectiveness in the actuator with magnitude 45%, $F_a = -0.45$ in $t = 4.5$ s is considered. A translational velocity variation from

1 to 1.6 m/s is applied using the same initial conditions in x and $\hat{x}$ mentioned in section 8.2. For this test, an increasing translational velocity were considered, in order to evaluate the proposed observer and system stabilization design. The results obtained in this case lead to interpretations analog to those perceived in the previous faulty case. It is possible to see, from Figure 12a), that the fault condition generates a strong inference in the closed-loop system presented in y_δ output due to the fault magnitude.

FIGURE 9

In Figure 12c) the control law, after the actuator fault, presents a variation from the equilibrium, caused by the fault magnitude. The Figure 10a) show the applied actuator fault and its correctly estimation. The actuator fault estimation e_f, finally, is depicted in Figure 10b).

FIGURE 10

8.5. Closed-loop simulation with time varying actuator fault

As a final test, a time varying actuator fault is considered. As said in previous sections, the most difficult task for the proposed observer consists in guarantee the state estimation error e_e convergence despite on the fault magnitude. With this in mind, the proposed observer should be evaluated under a time-varying actuator fault occurrence. The Figure 11a) and 11b) shows the real and estimated output y_δ and $y_{\dot{\phi}}$, respectively. The control law can be seen in Figure 11c) and, finally, 11d) show the translational velocity considered. The real and estimated fault, on the other hand, are depicted in Figure 12a), while the actuator fault estimation error $e_f = f_a - \hat{f}_a$ can be seen in Figure 12b).

FIGURE 11

From Figure 12b), it can be seen a small variation from 0 for the actuator estimation error e_f. The previous can be concluded from the fact that there is not an additional condition imposed in the observer design. In other words, the classical linear system theory stipulate that there is a error in the case of tracking references using **integer** actions. Despite this fact, the proposed observer design is able to maintain its stability in spite of any actuator fault type.

FIGURE 12

9. Conclusions

The results presented in this paper correspond to the design of an observer which is simultaneously in charge of the actuator fault and state estimation using a riderless bicycle polynomial LPV model. Taking the translational velocity of the bicycle as a parameter varying along the system trajectories, the observer is able to estimate the state and the actuator fault despite a BIAS, loss of effectiveness o time-varying fault occurrence. As an additional condition, the estimation comes with less noise than the actual system output measurements and, as a result from the test carried out, the correct performance for the proposed observer can be concluded. It is important to point out that with the proposed design, a versatile observer is generated, allowing to generate a stabilizing control signal with a less-noise estimated state (with respect to the presented in the system outputs). Moreover, the actuator fault estimation can be used in the FTC framework. The efficiency and usefulness

of the proposed observer —which may be considered the main contribution of the present work— has been corroborated through simulations considering BIAS, loss of effectiveness and time-varying faults.

References

Alwi, H., Edwards, C., Marcos, A. (2012). "Fault reconstruction using LPV sliding mode observer for a class of LPV systems", *Journal of the Franklin Institute*, 349(2), pp. 510–530.

Andreo, D., Larsson, M., Cerone, V., Legruto, D. (2010). "Stabilization of a riderless bicycle: A Linear Parameter Varying Approach", *IEEE Control Systems Magazine*, 30, pp. 23–32.

Bara, G.I., Daafouz, J., Ragot, J., Kratz, F. (2000). "State estimation for affine LPV systems", *Decision and Control, 2000. Proceedings of the 39th IEEE Conference on*, 5, pp. 4565-4570.

Chilali, M., Gahinet P. (1996). "H_∞ Design with Pole Placement Constraints: An LMI approach", *IEEE Trans. on Automatic Control*, 41(3), pp. 358–367.

Gilbert, W., Henrion D., Bernussou, J., Boyer D. (2010). "Polynomial LPV synthesis applied to turbofan engines", *Control Engineering Practice*, 18(9), pp. 1077–1083.

Gonzalez, A.M., Hoffmann, C., Radisch, C., Werner, H. (2013). "LPV observer Design and Damping Control of Container Crane Load Swing", *Control Conference (ECC), 2013 European*, pp. 1848 – 1853.

Khedher, A., Othman, K. B. (2010). "Proportional Integral Observer Design for State and Faults Estimation: Application to the Three Tanks System", *International Review of Automatic Control (I.RE.A.CO)*, 3(2), pp. 115-124.

Lofberg, J., Lab. of Autom. Control, Eidgenossische Tech. Hochschule, Zurich (2009). "YALMIP: a toolbox for modeling and optimization in MATLAB", *IEEE International Symposium on Computer Aided Control Systems Design*, pp. 284-289.

Patton, R.J., Klinkhieo, S. (2010). "LPV fault estimation and FTC of a two-link manipulator", *American Control Conference (ACC), 2010*, pp. 4647-4652.

Rodrigues, M., Sahnoun, M., Theilliol D., Ponsart J-C. (2013). "Sensor fault detection and isolation filter for polytopic LPV systems: A winding machine opplication", *Journal of Process Control*, 23(6), pp. 805–816.

Poussot-Vasal, C., Sename, O., Dugard, L., Gáspar, P., Szabó, Z., Bokor, J. (2008). "A new semi-active suspension control strategy through LPV technique", *Control Engineering Practice*; 16(12), pp. 1519–1534.

Prajna, S., Wu, F. (2005). "SOS-based solution approach to polynomial LPV system analysis and synthesis problems", *International Journal on Control*, 78(8), pp. 600-611.

Rotondo, D., Nejjari, F., Torren, A., Puig, V. (2013). "Fault Tolerant Control Design for Polytopic Uncertain LPV Systems: Application to a Quadro-

tor", *Control and Fault-Tolerant Systems (SysTol), Conference on*; pp. 643 – 648.

Rugh, W.J., Shamma, J.S. (2000). "Research on Gain Schedulling", *Automatica*; 36, pp. 1401–1425.

Schwab, A. L., Meijaard, J. P., Papadopoulos, J. M. (2005). "Benchmark results on the linearized equations of motion of an uncontrolled bicycle", *International Journal of Mechanical Science and Technology*, 19(1), pp. 292–304.

Tuan, H. D., Apkarian P. (1999). "Relaxation of parameterized LMIs with control applications", *Int. J. of Robust and Nonlinear Control*, 9, pp. 59–84.

Zhang Y., Jiang, J. (2008). "Bibliographical review on reconfigurable fault tolerant control", *Annual Reviews in Control*, 32(2), pp. 229–252.

Briat C. (2008). "Commande et Observation Robustes des Systèmes LPV Retardés". PhD Thesis. Grenoble INP, 2008.

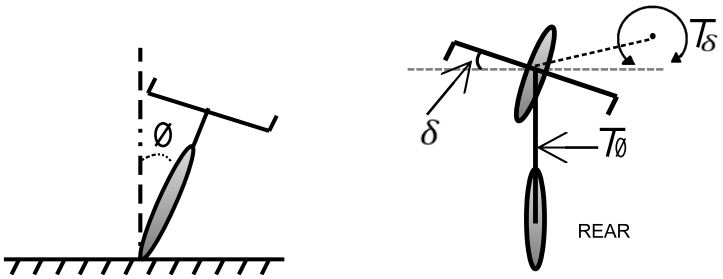

Figure 1: a) Front view of the bicycle and roll angle ϕ. b) Top view of the bicycle: handlebar angle δ and forces f

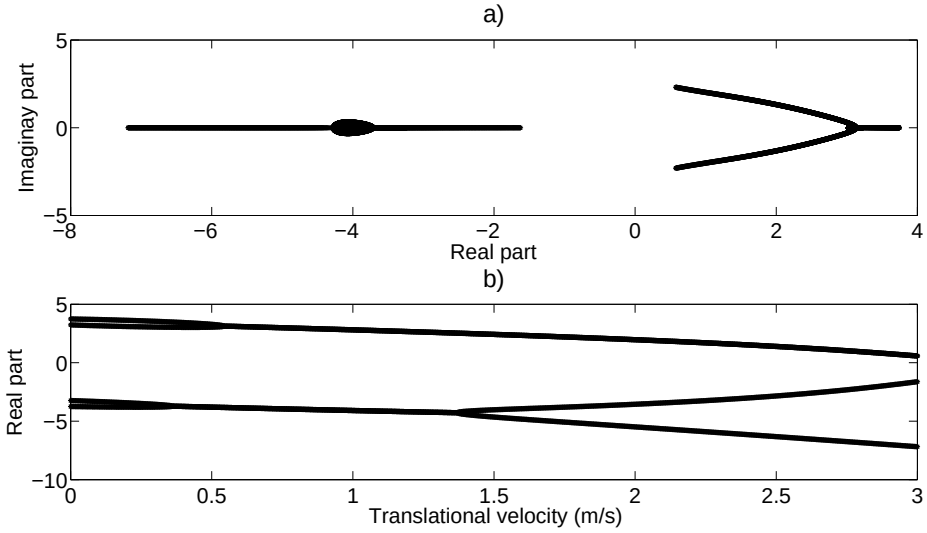

Figure 2: a) Open-loop eigenvalues; b) real part of open-loop eigenvalues in function of v

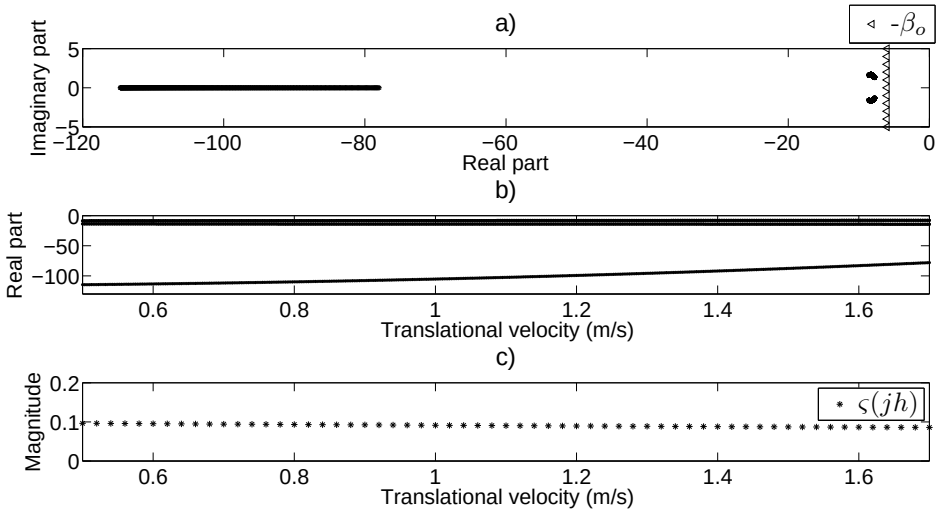

Figure 3: a) Observation error eigenvalues; b) real part of eigenvalues in function of v; c) parameter-varying attenuation level

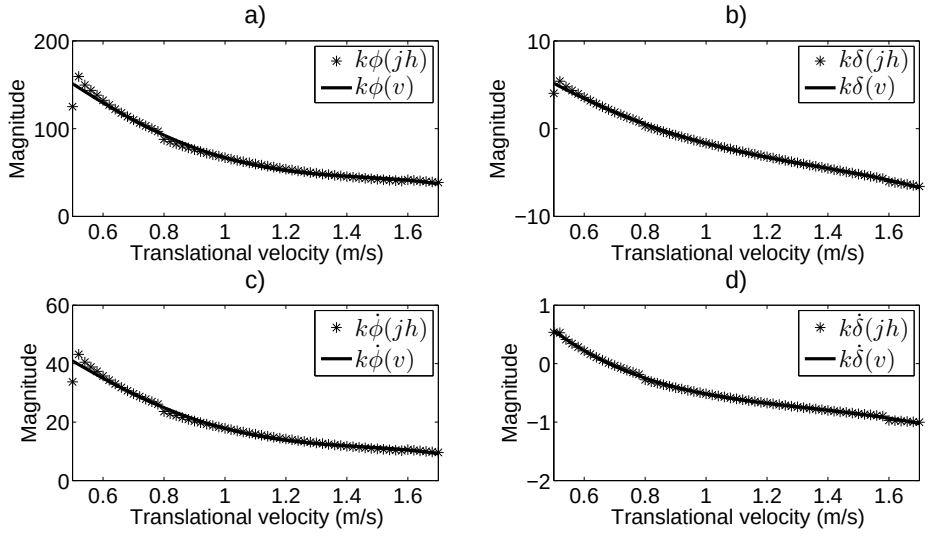

Figure 4: Discrete and interpolated controller gains. a) $k(\phi)$; b) $k(\delta)$; c) $k(\dot{\phi})$; d) $k(\dot{\delta})$

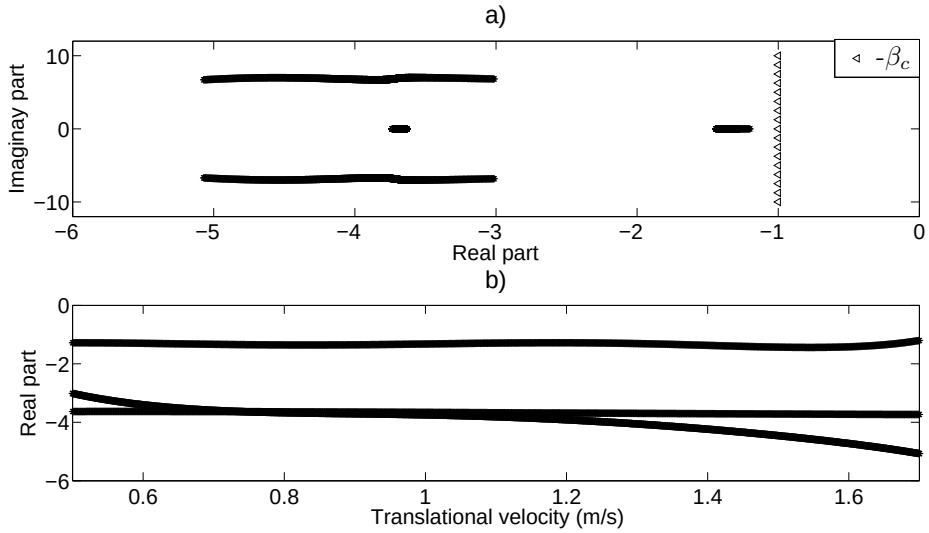

Figure 5: a) Closed-loop eigenvalues; b) real part of closed-loop eigenvalues in function of v

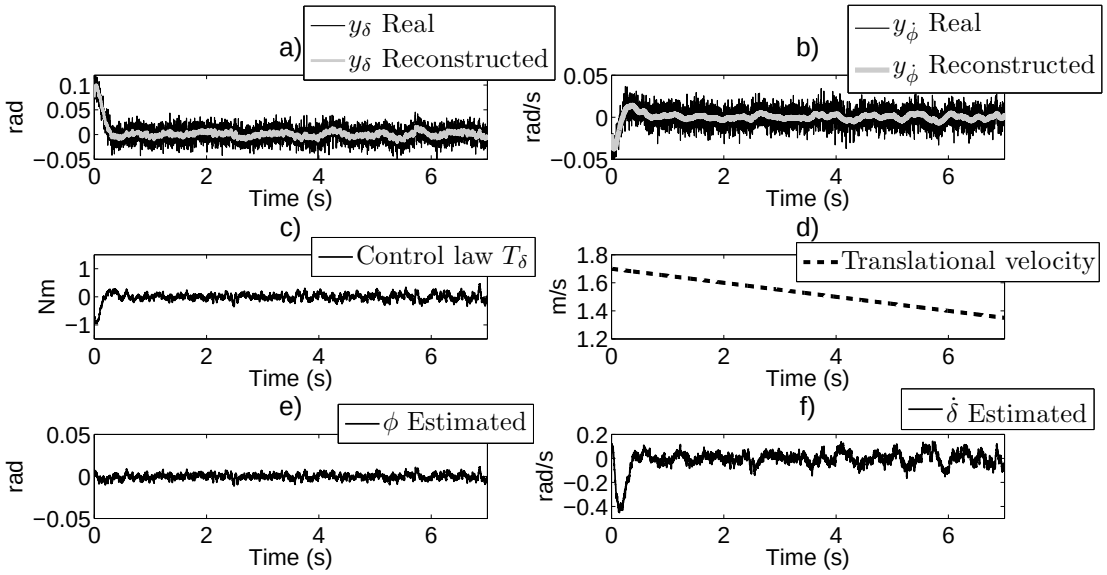

Figure 6: a) Real and estimated output y_δ; b) real and estimated output $y_{\dot\phi}$ c) translational velocity variation

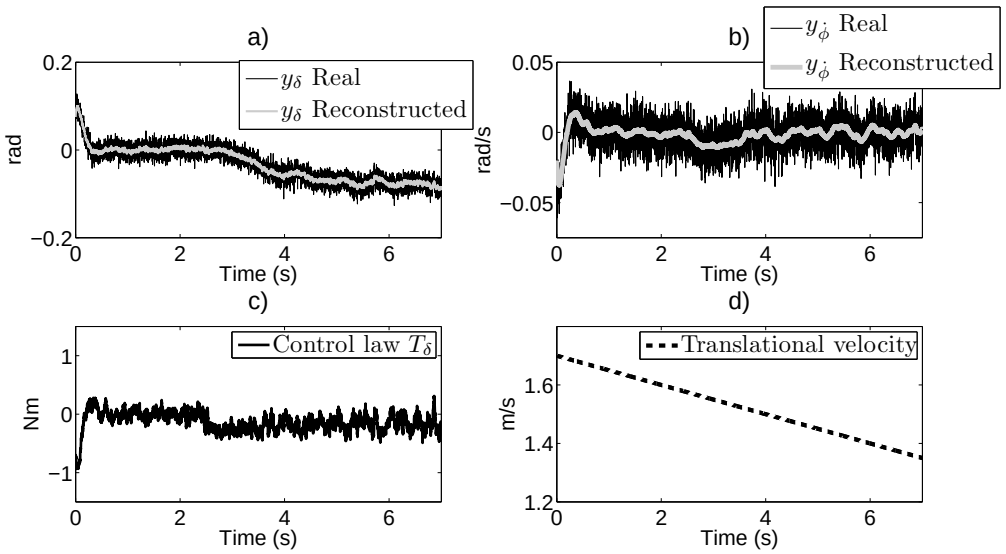

Figure 7: a) Real and estimated output y_δ; b) real and estimated output $y_{\dot{\phi}}$; c) translational velocity variation

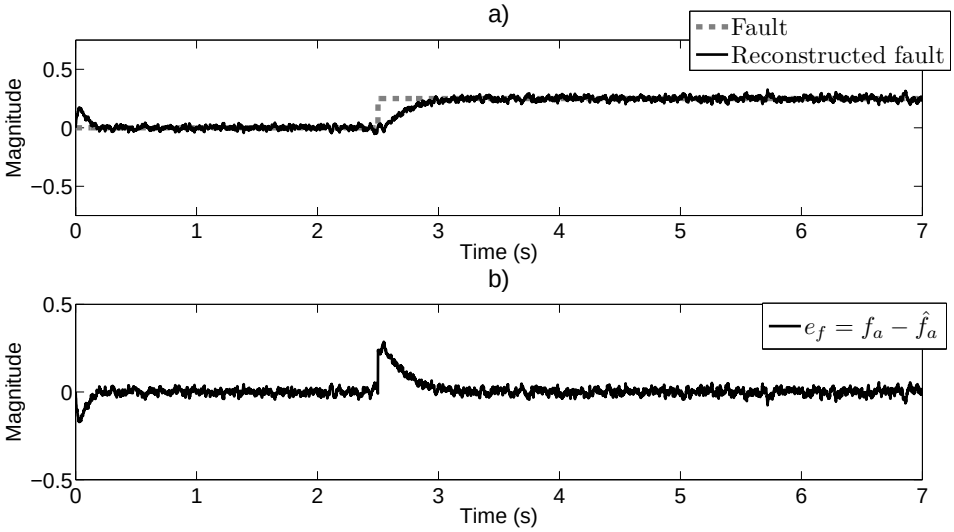

Figure 8: Real and actuator fault estimation

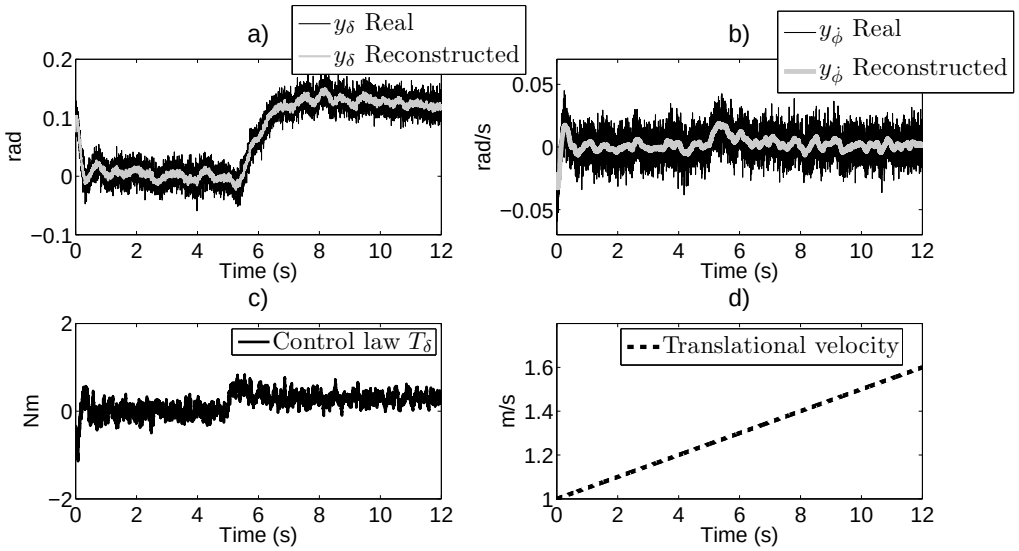

Figure 9: a) Real and estimated output y_δ; b) real and estimated output $y_{\dot{\phi}}$; c) translational velocity variation

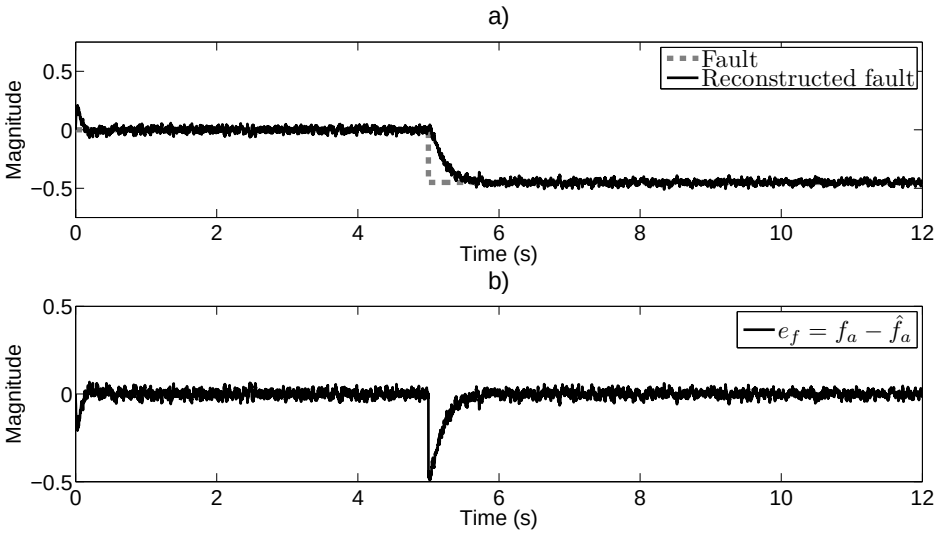

Figure 10: Real and actuator fault estimation

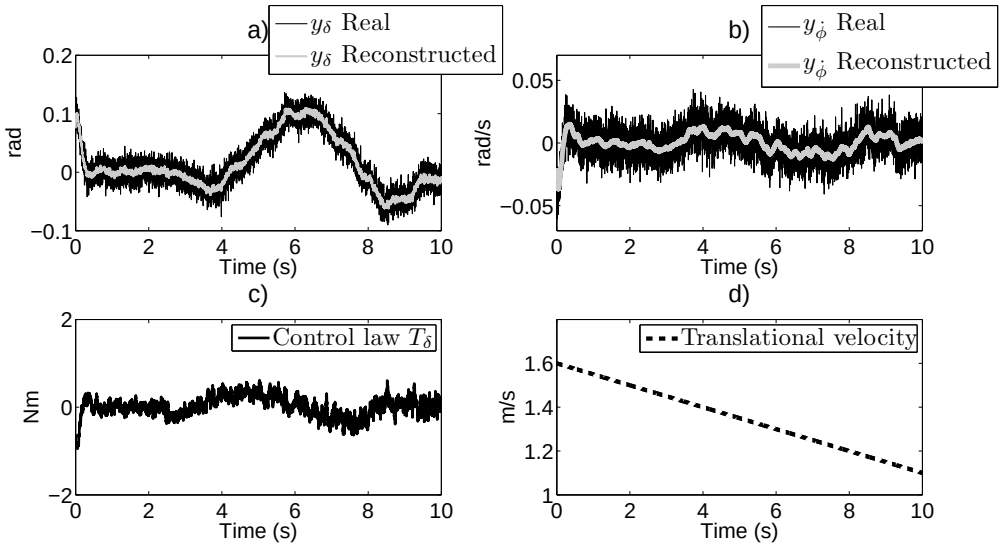

Figure 11: a) Real and estimated output y_δ; b) real and estimated output $y_{\dot{\phi}}$; c) translational velocity variation

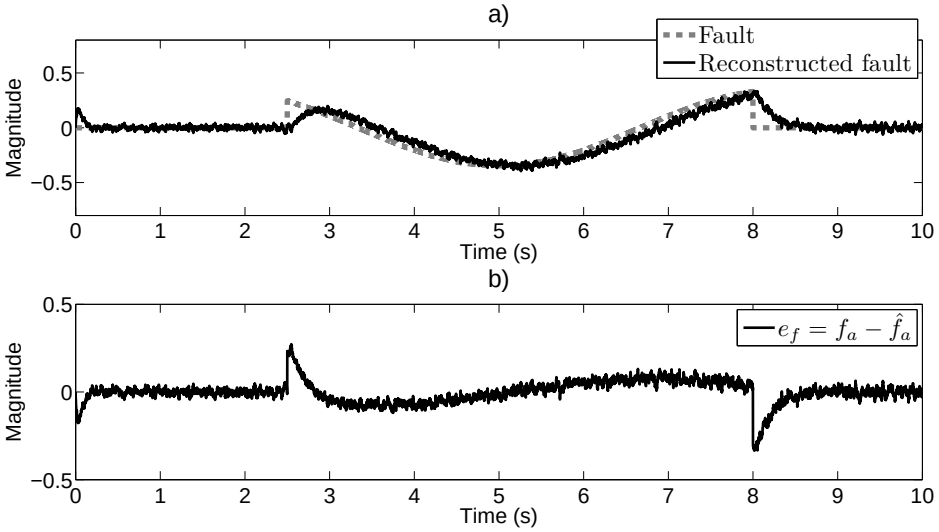

Figure 12: Real and actuator fault estimation